



Contents lists available at ScienceDirect

Marine Pollution Bulletin

journal homepage: www.elsevier.com/locate/marpolbul

Magnetic assessment and pollution status of beach sediments from Kerala coast (southwestern India)

Marcos A.E. Chaparro^{a,*}, G. Suresh^b, Mauro A.E. Chaparro^c, V. Ramasamy^d, M. Sundarajan^e

^a Centro de Investigaciones en Física e Ingeniería del Centro de la Provincia de Buenos Aires (CIFICEN, CONICET-UNCPBA), Pinto 399, 7000 Tandil, Argentina

^b Department of Physics, Theivanai Ammal College for Women (Autonomous), Villupuram, Tamilnadu, India

^c Centro Marplatense de Investigaciones Matemáticas (CEMIM-UNMDP-CONICET), Diagonal J. B. Alberdi 2695, Mar del Plata, Argentina

^d Department of Physics, Annamalai University, Tamilnadu, India

^e Department of Physics, Sri Chandrasekharendra Saraswathi Viswa Mahavidyalaya, Enathur, Kanchipuram, Tamilnadu, India

ARTICLE INFO

Article history:

Received 18 July 2016

Received in revised form 31 December 2016

Accepted 23 January 2017

Available online xxxxx

Keywords:

Beach sediments

Environmental magnetism

Mixture of magnetite/hematite

Multivariate statistical analyses

Pollution

ABSTRACT

Natural and anthropogenic activities along the coastal region of densely populated Kerala may introduce hazardous components into the coastal environment. The present study aimed to investigate the sources and impacts of hazardous components in beach sediments by environmental magnetism methods as additional tools. Magnetic parameters (such as mass-specific magnetic susceptibility $\chi = -1.2\text{--}154.4 \times 10^{-8} \text{ m}^3 \text{ kg}^{-1}$) and ratios that describe the magnetic properties of minerals such as Fe-oxides, indicate variable concentration of mixtures of magnetite and hematite (magnetite/hematite). The direct significant relationships between the variables indicate that higher concentration magnetic parameters are associated with higher radionuclides and metal contents. Magnetic properties and multivariate statistical analyses evidence the presence of contrasting groups defined only using a reduced number of magnetic variables. One of these groups, the central area of the Kerala coastline, showed the highest magnetic concentrations of mixtures of magnetite/hematite and higher values (up to 6.7) of pollution load index because of extensive anthropogenic activities.

© 2017 Elsevier Ltd. All rights reserved.

1. Introduction

Coastal sediments act as reservoirs of materials that are derived from both anthropogenic and natural weathering processes (Song et al., 2014). The Kerala coastal area in southwestern India is one of the sensitive coastal areas in India with rapid population growth and expanding industrial activities since the 1980s. It is one of the world's high-level background radiation areas. Natural radiation level in the region is higher than normal. This high-level radiation is believed to originate from rich deposits of monazite-bearing beach sand. The mineral monazite contains radioactive elements, which are the main cause for natural radiation in the southwestern coastal belt of India (Singh et al., 2007). In addition, this coastal ecosystem has been influenced by wide industrialized communities and extensive urbanized activities. Furthermore, this coastal belt continuously receives substantial loadings of heavy metals from river discharges, inlets, and estuaries that discharge runoff from adjacent land areas. Heavy metals in coastal sediments originate from the physical and chemical weathering of parent rocks, wastewater discharge, and atmospheric deposition. The accumulation and mobility of heavy metals in coastal sediments is influenced by various factors

such as the nature of the sediment particles, properties of adsorbed compounds, metal characteristics, and organic matter (Bastami et al., 2014).

Knowledge and detailed understanding of the various hazardous components are essential for monitoring the environmental changes caused by natural background radiation (radioactive elements) and anthropogenic activities (particulate matter, heavy metals, magnetic minerals, etc.) (El-Bahi, 2004; El-Gamal et al., 2007; Evans and Heller, 2003).

Magnetic measurements in environmental magnetism have been performed since the 1980's (Thompson and Oldfield, 1986) as additional tools to investigate the level of natural and anthropogenic activities in different ecosystems such as soils, estuaries, lakes, and rivers (Yang et al., 2007; Blundell et al., 2009; Horng et al., 2009; Zhang et al., 2011; Chaparro et al., 2015a; Prajith et al., 2015). Some authors have applied multivariate statistical analyses including principal components, cluster, canonical correlation, fuzzy c-means, and linear discriminant analysis to validate the relationship between the magnetic, radionuclide, and chemical variables and to classify the number of data points according to the similarities (Petrovský et al., 2001; Hanesch et al., 2001; Wang and Qin, 2006; Chaparro et al., 2008a, 2012, 2015b).

In the past years, rivers from south India have been studied using environmental magnetism, and such studies have focused on the magnetic properties of sediments and their relationship with radionuclides and heavy metals to assess the health of the riverine environment

* Corresponding author at: Instituto de Física Arroyo Seco (UNCPBA), Pinto 399, B7000GHG Tandil, Argentina.

E-mail address: chaparot@exa.unicen.edu.ar (M.A.E. Chaparro).

(Ramasamy et al., 2006, 2014a; Chaparro et al., 2008b, 2011, 2013, 2015a; Suresh et al., 2011; Krishnamoorthy et al., 2014). Among these studies, Ramasamy et al. (2014a) and Suresh et al. (2011) had reported significant correlations between χ (mass-specific magnetic susceptibility) and the concentrations of ^{232}Th , ^{238}U , and ^{40}K . In Bharathapuzha River (Kerala state), Krishnamoorthy et al. (2014) had also reported significant correlations between χ and the concentrations of ^{226}Ra and ^{40}K . They found that higher concentrations of both radionuclides may be associated with the extensive exploitation of phosphate and potassium fertilizers in the surrounding agricultural area.

The present study focuses on the magnetic properties of Fe-oxides present in the beach sediments collected from the Kerala coastline (southwestern India). The aim of the present work was to (a) characterize the magnetic particles in beach sediments, (b) determine the possible differences in the composition of magnetic minerals from surface to deeper layers (vertical distribution), (c) identify polluted sites along the coast using the magnetic properties of sediments, and finally (d) study the relationship between magnetic minerals, radionuclides, and heavy metals to confirm the use of magnetic parameters as environmental proxies.

2. Materials and methods

2.1. Study area

Kerala is the most densely populated state in India, with a population of 33.3 million (2011 census), and approximately 80% (27.4 million) of the population is living in the coastal zone. The coastal population density in major urban centers such as Cochin, Trivandrum, Calicut, Alleppey, and Quilon exceeds 2000 persons per sq. km. Kerala has a coastline length of approximately 560 km. The coastal region includes 27 estuaries and 7 lagoons. There are approximately 300 large- and medium-scale industries and 1,66,000 small-scale industries, most of which are located in the coastal area. Moreover, a major port at Cochin and 14 minor ports and fishing harbors are situated in this coastal zone (Ramasamy et al., 2013).

Kerala has a total of ten coastal districts; the present study area covers four coastal districts: Ernakulam, Alappuzha, Kollam, and Trivandrum. The hydrodynamic regime of the coastal marine zone of Kerala depicts the typical features of a monsoon-dominated tropical coast. The highest wave and current intensity occurs during the peak monsoon months of June–July. The near shore wave intensity decreases from south to north. The longshore currents generated by the waves are generally southerly during monsoon (Ramasamy et al., 2013).

2.2. Sampling

The study area covers a total coastline length of approximately 200 km, where 39 successive sampling sites were selected and numbered as S1–S39 (from $9^{\circ}57'49''\text{N}$, $76^{\circ}14'16''\text{E}$ to $8^{\circ}34'21''\text{N}$, $76^{\circ}50'09''\text{E}$) (Fig. 1). The latitudinal and longitudinal position of the sampling sites were determined using a hand-held global positioning system (GPS) (Model: GARMIN GPS-12) unit. Consecutive neighboring sites were separated by a distance of approximately 4–5 km (Ramasamy et al., 2013).

The samples were collected at a distance of 5–10 m from the high tide mark at four different depths: from the upper layer (0–5 cm depth), the 1 ft below the surface, the 2 ft below the surface, and the 3 ft below the surface. Samples were collected using a plastic spade during the summer of 2011, and the collected samples were placed in polyethylene bags. The total weight of the collected samples was approximately 3 kg. In the laboratory, the collected samples were dried at room temperature in open air for a few days. Then, the dry samples were sieved (2 mm) to remove gravel fraction and packed and stored in polyethylene bags (Suresh et al., 2015).

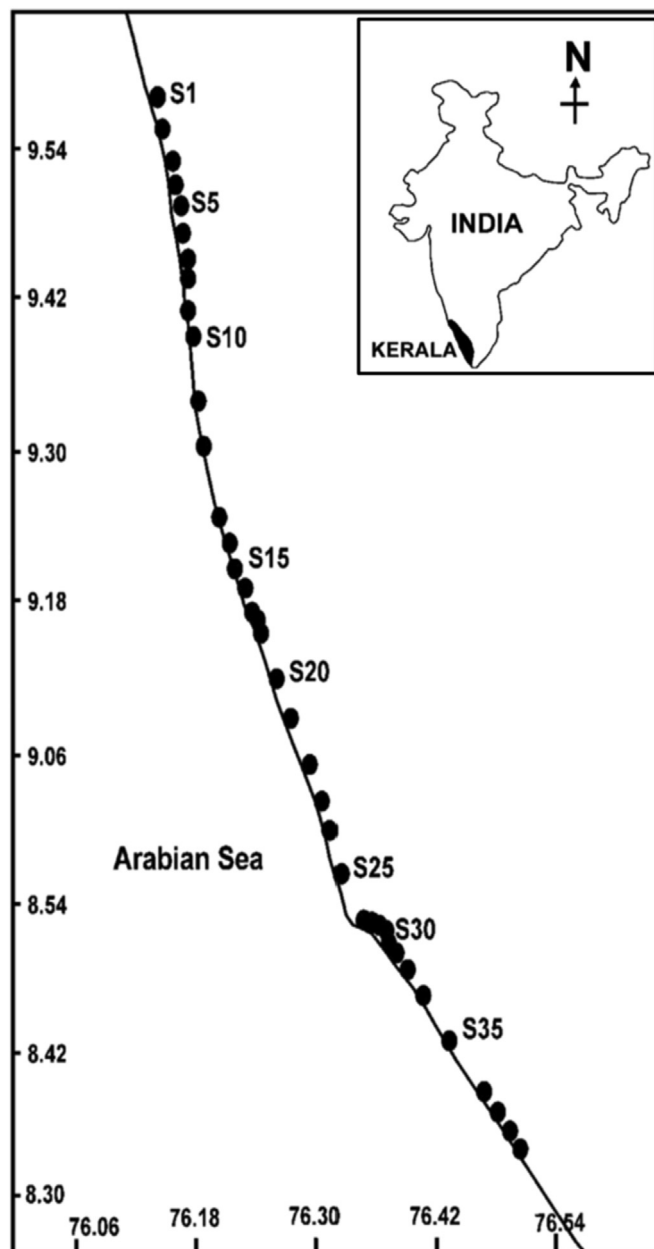


Fig. 1. Map of the study area in Kerala. Beach sediments were collected from sites along the coast.

2.3. Magnetic measurements

The air-dried samples were subsampled for magnetic studies using plastic containers (approximately 2.3 cm^3). They were then packed, weighed, and labeled. Subsequently, all samples were fixed using sodium silicate to prevent unwanted movement when studying remanent magnetization.

Magnetic susceptibility was measured using the magnetic susceptibility meter MS2 (Bartington Instruments Ltd., 1994) linked to the MS2B dual frequency sensor (0.47 and 4.7 KHz). The volumetric susceptibility (κ) and mass-specific susceptibility (χ) were computed.

Anhyseretic remanent magnetization (ARM) was determined using a device attached to a shielded demagnetizer (Molspin Ltd.), superimposing a DC bias field of $90\text{ }\mu\text{T}$ (71.6 A/m) to a peak alternating field (AF) of 100 mT in the AF interval 100–2.5-mT and an AF decay rate of $17\text{ }\mu\text{T}$ per cycle. The remanent magnetization was measured using a

spinner fluxgate magnetometer (Minispin, Molspin Ltd.). Anhyseretic susceptibility (volume κ_{ARM} and mass-specific χ_{ARM}) was estimated by linear regression for ARM acquired at different DC bias fields of 10, 60, and 90 μT (7.96, 47.7, and 71.6 A/m). The $\kappa_{\text{ARM}}/\kappa$ and King's plot (χ_{ARM} versus χ , King et al., 1982) were also studied.

The isothermal remanent magnetization (IRM) acquisition studies were performed using a pulse magnetizer, model IM-10-30 (ASC Scientific). Each sample was magnetized by exposing it to stepwise growing DC fields from 4.3 to 2470 mT. The remanent magnetization after each step was measured using the abovementioned magnetometer Minispin. In these measurements, IRM acquisition curves and the saturation of IRM ($\text{SIRM} = \text{IRM}_{2470 \text{ mT}}$) were determined using forward DC fields. Remanent coercivity (H_{cr}), S-ratios ($S_{-300} = -\text{IRM}_{-300 \text{ mT}}/\text{SIRM}$; $S_{-100} = -\text{IRM}_{-100 \text{ mT}}/\text{SIRM}$), HIRM [$=0.5 \times (\text{SIRM} + \text{IRM}_{-300 \text{ mT}})$], and L-ratio [$=(\text{SIRM} + \text{IRM}_{-300 \text{ mT}})/(\text{SIRM} + \text{IRM}_{-100 \text{ mT}})$] were also calculated using backfield measurements once the SIRM was reached.

2.4. Radionuclides and PLI of metals data

The surface (0–5 cm) beach sediment samples ($n = 39$) were subsampled and prepared according to the protocol, and activity concentrations of ^{238}U , ^{232}Th , and ^{40}K (gamma ray spectrometer) were measured as reported by Ramasamy et al. (2013). The below detectable limit for each radionuclide is 5.5 Bq kg^{-1} for ^{238}U and ^{232}Th and 21.5 Bq kg^{-1} for ^{40}K .

The level of heavy metals (Cd, Cr, Cu, Ni, Pb, and Zn) in and pollution load index (PLI; Tomlinson et al., 1980) of all layer samples were reported by Suresh et al. (2015). The concentrations of the abovementioned radionuclides and heavy metal data were obtained from Ramasamy et al. (2013) and Suresh et al. (2015), respectively, to make a correlation with magnetic parameters.

2.5. Statistical methods

Statistical analyses of the dataset were performed to determine whether there are (a) significant differences in the values of each magnetic parameter with depth and between sites; (b) relationships between magnetic parameters, radionuclide variables, and the PLI; and (c) samples with similar magnetic properties to allow contrasting grouping of sites along the coastline. Multivariate statistical analyses were performed using the R free software: R version 3.2.2 (R Core Team, 2015).

To determine significant differences between depth levels (0, 30, 60, and 90 cm) for each magnetic parameter, the Friedman's test (or Friedman's ANOVA) was applied for all magnetic parameters. This test is a non-parametric version of ANOVA for repeated measures; it is used to detect differences in treatments across multiple test attempts. The Friedman's test is used for one-way repeated measures ANOVA by ranks.

The relationship between the magnetic parameters, radionuclides, and PLI were analyzed by principal component analysis (PCA) with matrix correlation. Before the PCA, the measure of sampling adequacy (MSA) of factor-analytic data matrices was estimated. This value indicates whether it is appropriate to apply PCA for the dataset matrix. In addition, a nonhierarchical k-means clustering (CA) with Euclidean distance was performed. The coordinates of the rows obtained from the PCA were used to build the clusters.

3. Results and discussion

3.1. Magnetic minerals in beach sediment

Values of mass-specific susceptibility ranged between -1.2 and $154.4 \times 10^{-8} \text{ m}^3 \text{ kg}^{-1}$ (values of magnetic susceptibility and other magnetic parameters of all sites are given in Supplementary Data). The variation in the values indicates the presence of changes not only

in the magnetic concentration of minerals but also in the magnetic mineralogy. Approximately a half ($n = 73$) of the beach samples showed χ values below $10.0 \times 10^{-8} \text{ m}^3 \text{ kg}^{-1}$, indicating that the magnetic signal is possibly regulated by diamagnetic/paramagnetic minerals, i.e., there is a dominance of diamagnetic/paramagnetic minerals over ferrimagnetic and antiferromagnetic ones (Dearing, 1999). Among the diamagnetic minerals, quartz and calcite were the main minerals found in these beach sediments as the amount of major light minerals decreased in the order quartz > calcite > microcline feldspar > kaolinite (Ramasamy et al., 2014b).

Such values are, in this sense, interpreted as a first approach of the presence of mineral mixtures and relative contribution of the main magnetic mineral categories: diamagnetic, paramagnetic, and ferrimagnetic/antiferromagnetic. As observed from the remanent magnetic parameters in Fig. 2 (χ_{ARM}) and Fig. 3 (HIRM, H_{cr} and ARM/SIRM), a small amount of ferrimagnetic and antiferromagnetic minerals were also present in these 73 samples (S2, S4–S12, S19, S30–S33, and S35–S39), which included 10 samples with negative values of mass-specific susceptibility.

Presence of mixtures of ferrimagnetic (magnetite Fe_3O_4) and antiferromagnetic (hematite Fe_2O_3) minerals, i.e., magnetite/hematite, were confirmed from the analysis of IRM curves and a wide variation in remanent coercivity values (31.6–267.8 mT). Presence of softer (magnetite) and higher (hematite) coercivity minerals can be predicted from their characteristic values (e.g., Peters and Dekkers, 2003). In the present study, the quartile values (Q1–Q3) were 60.5–122.4 mT, and the median value of H_{cr} was 99.9 mT. The remanent coercivity of natural samples composed of ferrimagnetic and antiferromagnetic mineral mixtures depends on their contribution. As shown by Chaparro and Sinito (2004), the H_{cr} values can vary widely according to the hematite and magnetite ratio, e.g., $H_{\text{cr}} = 605.5 \text{ mT}$ (for 420:1, 420 parts of hematite per one part of magnetite) and $H_{\text{cr}} = 57.2 \text{ mT}$ (for 110:1). Among these magnetic minerals, the quantity of magnetite and ilmenite were determined by Ramasamy et al. (2014b) as the main heavy minerals after the most abundant mineral monazite in such samples. Although hematite was not observed in those samples, it is possible that this mineral was not distinguished in mixtures of magnetite/hematite or in ilmenite/hematite minerals.

The S-ratio is a measure of the relative abundance of high-coercivity minerals in a mixture containing ferrimagnetic minerals. The beach sediments in the present study showed a relative variation of both minerals, which could be observed from the S-ratio values that ranged

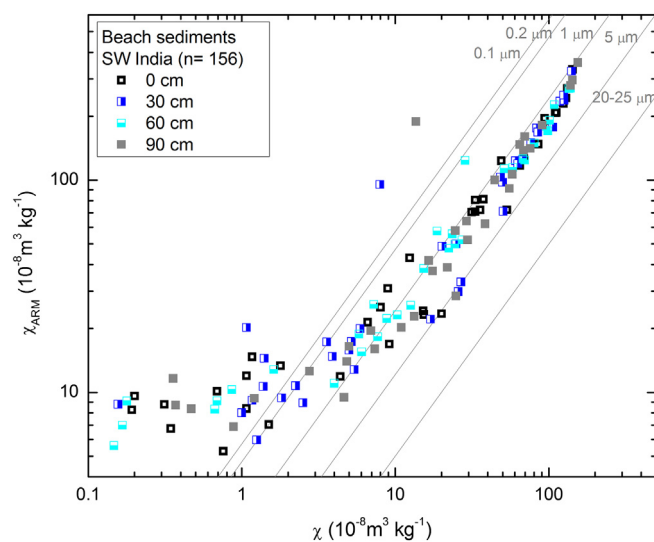


Fig. 2. The King's plot (χ_{ARM} vs. χ) for beach samples. As a general trend, samples with higher magnetic concentration-dependent parameters showed coarser magnetic grain sizes.

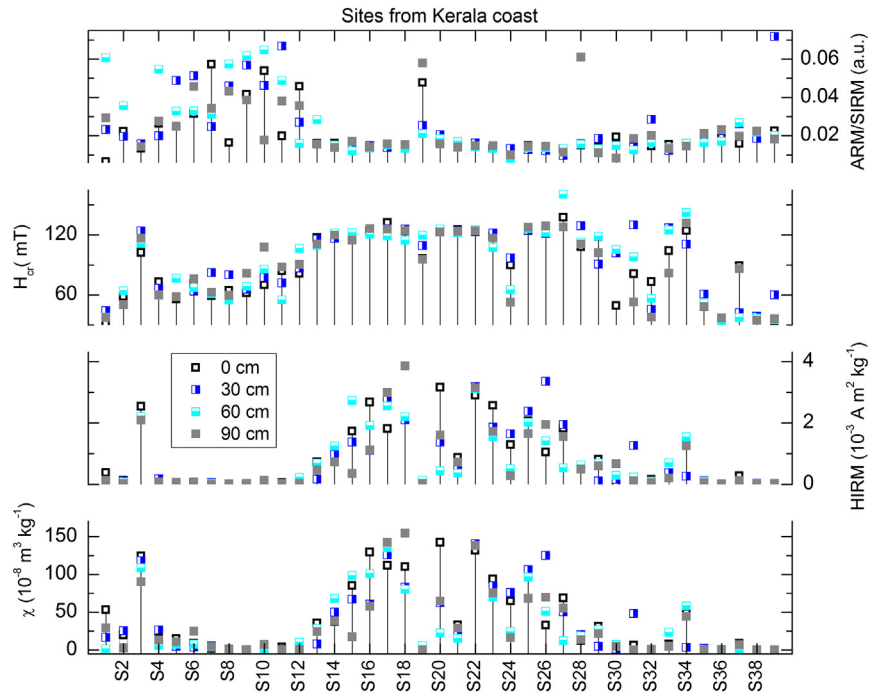


Fig. 3. Spatial distribution of concentration - (χ and HIRM) and mineralogy-dependent (H_{cr} and ARM/SIRM) magnetic parameters for different depths.

(S_{-300}) from 0.58 to 0.76. As detailed in Fig. 4, the S-ratio statistically correlates with H_{cr} . HIRM is used as a measure of the mass concentration of high-coercivity magnetic minerals such as hematite (Liu et al., 2012). In the present study, because HIRM is not correlated with the L-ratio and the latter is relatively stable (L-ratio = ~0.36), it is expected that these HIRM values indicate a variation in the concentration of high-coercivity minerals.

The grain size of magnetite minerals varied between 1 and 5 μm for samples with higher magnetic concentration ($\chi > 10 \times 10^{-8} \text{ m}^3 \text{ kg}^{-1}$) (Fig. 2), and finer magnetic grains of 0.2–1 μm and <0.1 μm were observed for lower magnetic values of $\chi = 1.5\text{--}10 \times 10^{-8} \text{ m}^3 \text{ kg}^{-1}$ and $<1.5 \times 10^{-8} \text{ m}^3 \text{ kg}^{-1}$, respectively.

Results of other magnetic grain-size indicative parameters ARM/SIRM (Fig. 3) and κ_{ARM}/κ show a similar behavior, with a relative narrow variation, e.g., the Q1–Q3 of κ_{ARM}/κ was 1.8 – 4.7.

3.2. Magnetic variables, PLI, and natural radionuclides

The Friedman's test (or Friedman's ANOVA) was applied for all magnetic parameters revealing that there are no significant differences ($p < 0.001$) between depth levels from 0 to 90 cm. Because there were no significant differences between the depth levels, the statistical analyses were performed only for beach sediment samples from the surface level.

The bivariate analysis showed significant correlations between the magnetic variables, radionuclides ^{238}U and ^{232}Th , and the PLI. The concentration-dependent magnetic variables χ , ARM, SIRM, and HIRM were correlated with PLI and radionuclide variables. Significant correlations of magnetic variable were observed with PLI ($R = 0.480\text{--}0.527$) and ^{238}U ($R = 0.504\text{--}0.596$) and ^{232}Th ($R = 0.375\text{--}0.467$) ($p < 0.01$). Mineralogy-dependent magnetic variables were correlated with PLI and radionuclides. Moreover, ARM/SIRM and S-ratios (S_{-300} and S_{-100}) were inversely correlated with PLI and ^{238}U , and H_{cr} was directly correlated with ^{232}Th and ^{238}U .

Some investigations have shown a correlation between radionuclide concentrations and magnetic minerals (McCubbin et al., 2004; Montes et al., 2012). Suresh et al. (2011) found that χ is directly correlated with the concentration of ^{232}Th ($R = 0.603$) and inversely correlated with the concentration of ^{238}U . They found that the activity concentration depends on the composition of clay minerals (kaolinite). In addition, Ramasamy et al. (2014a) reported significant direct correlations between χ and the concentration of ^{232}Th ($R = 0.751$) and ^{238}U ($R = 0.774$) in Vaigai River. They showed that both correlated variables and the magnetic parameter could be controlled by a common mechanism. Furthermore, significant direct correlations between concentration-dependent magnetic variables and PLI were found not only in other studies in South India (Chaparro et al., 2011), but also in other pollution studies (Chaparro et al., 2015b). They documented the use of magnetic parameters to determine the PLI.

For multivariate analyses, the MSA was previously estimated to the PCA. The estimated MSA (0.76) indicated that it was appropriate to apply a PCA. The PCA with correlation matrix was performed for magnetic parameters (χ , ARM, SIRM, HIRM, ARM/SIRM, H_{cr} , S_{-300} , S_{-100}),

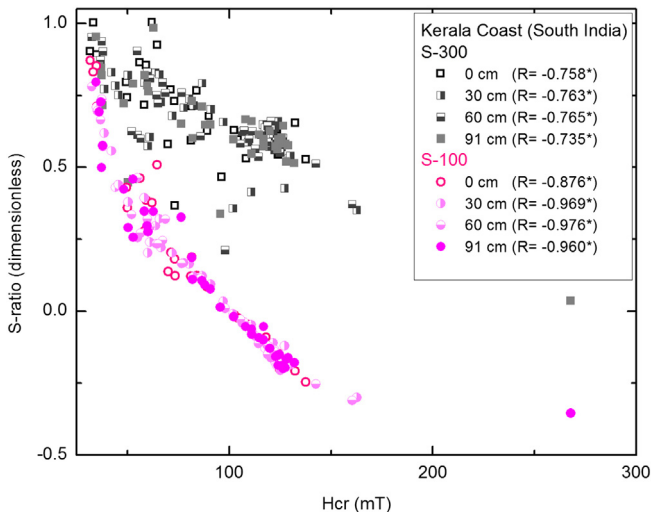


Fig. 4. Biplots using mineralogy-dependent parameters. S-ratios vs. H_{cr} .

radionuclides (^{238}U , ^{232}Th , ^{40}K), and PLI. The first three principal components (PCs) accounted for the 82% of the dataset variation. From the loading analysis of PC, loadings of variables $>0.75 * \max(\text{loading PC\#})$ were identified as the main contribution for each PC. It is worth to note that the first PC (PC1) is composed of the concentration magnetic parameters (χ , ARM, SIRM, HIRM, and H_{cr}). These parameters showed direct relationship and S_{-100} showed an inverse relationship, as observed in the plane PC1–2 in Fig. 5. In addition, the radionuclides ^{238}U and ^{232}Th and the PLI evidence a direct relationship in this plane. It is worth mentioning that the angle between the two variables on coordinate planes is an indicator of the correlation between the variables. Thus, the magnetic variables χ , ARM, SIRM and HIRM seem to correlate with the PLI, ^{238}U , and ^{232}Th . In the plane PC1–3, a direct (and inverse) relationship between ^{238}U and H_{cr} (S_{-300} and S_{-100}) can be observed; in addition, concentration-dependent magnetic variables seem to correlate with ^{238}U (Fig. 5).

These results support the use of concentration-dependent magnetic parameters as indicators of the PLI and concentration of radionuclides ^{238}U and ^{232}Th in beach sediments from Kerala coastline. Among these magnetic parameters, χ is a very good choice for assessing the PLI and concentration of ^{238}U and ^{232}Th because its measurements are easy, prompt, and cost-effective to perform (Petrovský and Ellwood, 1999).

3.3. Spatial distribution of magnetic parameters

The spatial variation of different concentration-dependent magnetic parameters, i.e., χ , ARM, SIRM, and HIRM, shows a similar pattern (Fig. 3), indicating that the highest values were present in the central part along the Kerala coast, i.e., in sites S13–S18, S20–S29, S1, S3, and S34. Such similarities between distribution patterns were also observed and supported by the CA (the central part corresponding to group G3, Fig. 6), and the correlation results between such concentration-dependent magnetic parameters were statistically significant ($p < 0.01$), with Pearson's coefficients varying between 0.95 and 0.99. The parameter χ showed a clear contrast between diamagnetic/paramagnetic ($\chi = -1.2\text{--}10.0 \times 10^{-8} \text{ m}^3 \text{ kg}^{-1}$) and ferrimagnetic/antiferromagnetic minerals according to the sites along the coast. This pattern is similar to the quartz distribution reported in these beach sediments by Ramasamy et al. (2014b). In general, the higher contents of quartz are in agreement with lower values of the parameter χ (Fig. 3) and vice versa. Although there is a clear difference of χ value between different magnetic mineral types, small amounts of ferrimagnetic/antiferromagnetic minerals are also present in samples with high diamagnetic/paramagnetic mineral content. Thus, it is interesting to note that the remanence parameters ARM, SIRM and HIRM are only dependent on the content of

ferrimagnetic/antiferromagnetic minerals and have a similar behavior to parameter χ .

Higher magnetic concentrations for all depth layers are mainly found in central sites (from S13 to S29) and correspond to the third quartile of magnetic parameters: χ (Q1–Q3 = $1.2\text{--}59.5 \times 10^{-8} \text{ m}^3 \text{ kg}^{-1}$), ARM (Q1–Q3 = $8.4\text{--}99.0 \times 10^{-6} \text{ A m}^2 \text{ kg}^{-1}$), SIRM (Q1–Q3 = $0.4\text{--}6.7 \times 10^{-3} \text{ A m}^2 \text{ kg}^{-1}$) and HIRM values (Q1–Q3 = $0.03\text{--}1.40 \times 10^{-3} \text{ A m}^2 \text{ kg}^{-1}$). Reported concentration of radionuclides (Ramasamy et al., 2013) and the pollution index PLI (Suresh et al., 2015) also show a similar pattern for surficial sediments in this central area. Higher values correspond to the third quartile of both, the pollution index PLI (Q1–Q3 = 2.69–4.53) and the radionuclides ^{238}U (Q1–Q3 = $9.3\text{--}195.2 \times \text{Bq kg}^{-1}$) and ^{232}Th (Q1–Q3 = $12.0\text{--}613.2 \times \text{Bq kg}^{-1}$).

Most of these central sites evidence a similar remanent coercivity values belonging to the Q3 ($H_{cr} = 122.4 \text{ mT}$, Fig. 3) in contrast with the other sites (with lower magnetic concentration) belonging to the Q1 ($H_{cr} = 60.5 \text{ mT}$). The distribution of such grains can be appreciated in Fig. 3 from the magnetic grain-size indicative parameter ARM/SIRM. Lower values of this parameter correspond to the 1st quartile (Q1 = 0.01) and indicate coarser magnetic grains in mineral mixtures (magnetite-hematite) that belong to the central sites (S13–S29) along the Kerala beaches. On the contrary, the finest magnetite grains are observed in sites S4–S12 and S19, and slightly finer in sites S30–S33 and S35–39 (3rd quartile of ARM/SIRM, Q3 = 0.03).

The existence of groups of surficial samples with similar features was analyzed by a CA (with Euclidean distance) where each cluster is characterized only by magnetic variables. Among the variables, the magnetic parameters χ , HIRM, ARM/SIRM and H_{cr} are presented in such CA. The sample set was partitioned into three groups made of 5 (G1), 17 (G2) and 17 (G3) samples characterized with different magnetic centroids (Table 1). These multivariate results support the observed spatial behavior of magnetic parameters as discussed above.

Group G3 is composed of the samples belonging to the central part of the coast (Fig. 6). These samples have the highest values of concentration-dependent magnetic parameters (e.g.: the centroid of $\chi = 81.4 \times 10^{-8} \text{ m}^3 \text{ kg}^{-1}$) as well as high coercivity minerals (centroid of $H_{cr} = 120.4 \text{ mT}$) and coarser magnetic grain sizes (lower values of ARM/SIRM). In contrast, samples corresponding to group G1 are characterized by the lowest values of concentration-dependent magnetic parameters and finer magnetic grain. Group G2 is composed of a half of total of samples comprising sites located on the southern part of the Kerala coast. Such samples show a relatively low concentration-dependent magnetic parameters (centroid of $\chi = 9.4 \times 10^{-8} \text{ m}^3 \text{ kg}^{-1}$), though they are characterized by low-coercivity minerals (centroid of $H_{cr} = 64.5 \text{ mT}$, Table 1).

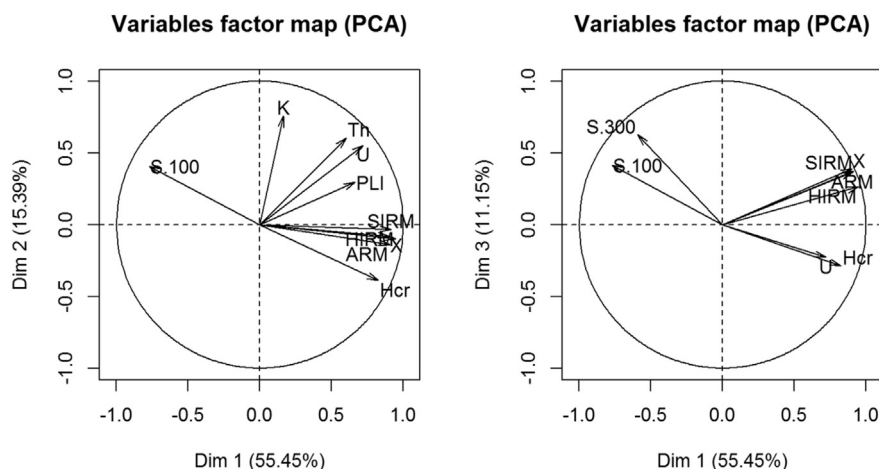


Fig. 5. Multivariate analysis (PCA) representation of the magnetic variables (magnetic concentration-dependent parameter: χ , ARM, SIRM and HIRM; magnetic mineralogy-dependent parameters: H_{cr} , S_{-300} and S_{-100} ; and magnetic grain size-dependent parameters: ARM/SIRM) and the PLI in the coordinate planes PC1–2 and PC1–3.

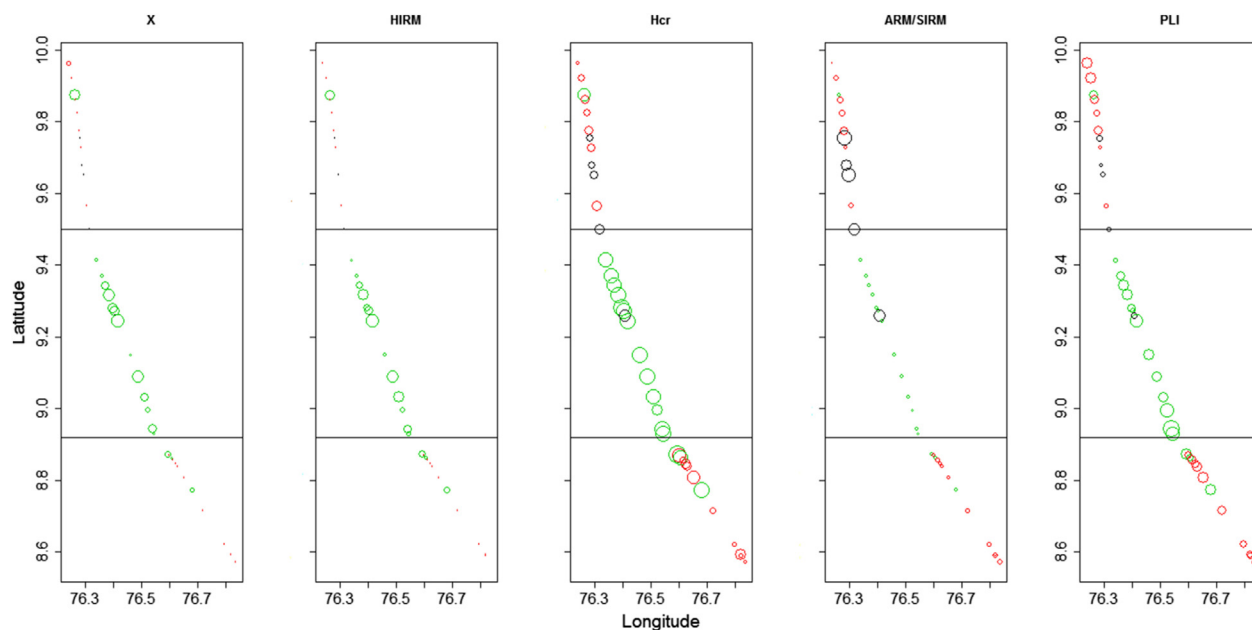


Fig. 6. Cluster analysis. Three groups were obtained using only magnetic parameters. Groups are highlighted in different colors: G1 in black, G2 in red, and G3 in green color. The size of the symbols is represented considering the standardized value of each sample with respect the range of corresponding variable (i.e., $3Spar(i)/(\max(Spar)-\min(Spar))$, where $Spar$ is the value of a variable for the i^{th} sample). (For interpretation of the references to color in this figure legend, the reader is referred to the web version of this article.)

4. Conclusions

An integrated analyses of magnetic parameters validate the presence of mixture of magnetite/hematite minerals in all the samples. This mixture varied widely among the beach sites because of the changes in magnetic concentration (χ varies between -1.2 and $154.4 \times 10^{-8} \text{ m}^3 \text{ kg}^{-1}$; $\text{HIRM} = 0.00\text{--}3.86 \times 10^{-3} \text{ A m}^2 \text{ kg}^{-1}$), magnetite and hematite mineral contribution ($S_{-300} = 0.03\text{--}1.00$; $H_{cr} = 31.6\text{--}267.8 \text{ mT}$) and magnetic grain sizes (between 0.1 and $5 \mu\text{m}$; e.g.: $\text{ARM/SIRM} = 0.01\text{--}0.08$). Although in some sites, the diamagnetic/paramagnetic mineral (quartz) contribution is dominant along with the small amount ferrimagnetic and antiferromagnetic minerals. The statistical analyses of all magnetic parameters revealed no significant differences ($p < 0.001$) observed in magnetic parameters between surface sediments and the other depth levels (30, 60, and 90 cm).

Because the magnetic parameters such as χ , ARM, SIRM, HIRM, and H_{cr} are statistically correlated with the pollution index PLI of metals and concentrations of natural radionuclides ^{238}U and ^{232}Th , the integrated magnetic methods can be a substitution for assessing the levels of heavy metals and radionuclide concentrations in beach sediments from coastlines similar to those of Kerala. Direct correlations among the variables are indicative of higher concentration of magnetic, radionuclides, and heavy metals. Among these magnetic parameters, χ is a good alternative method to assess these pollutants because susceptibility measurement is prompt, non-destructive, and cost-effective.

The CA shows that the central area (group G3) with the highest magnetic concentrations is characterized by coarser grains and by higher

contribution of hematite in mixtures of magnetite/hematite, and high concentrations of studied heavy metals and PLI values (PLI up to 6.7). In contrast, group G1 has lowest PLI values that are characterized by low magnetic concentrations and finer grains. The obtained relationship between magnetic parameters and PLI is re-confirmed with CA. Hence, the present study recommends that to make an accurate pollution assessment, magnetic susceptibility measurement can be used as a first approach and other magnetic parameters can be measured consequently and used for assessment.

Acknowledgements

The authors wish to thank the Annamalai University, Universidad Nacional del Centro de la Provincia de Buenos Aires (UNCPBA), and National Council for Scientific and Technological Research (CONICET) for their financial support. They also thank Mr. P. Zubeldia (Tech. CICPBA) for his help. This manuscript was improved by useful suggestions of anonymous reviewers.

Appendix A. Supplementary data

Supplementary data to this article can be found online at <http://dx.doi.org/10.1016/j.marpolbul.2017.01.044>.

References

- Bastami, K.D., Bagheri, H., Kheirabadi, V., Zaferani, G.G., Teymori, M.B., Hamzehpoor, A., Soltani, F., Haghparast, S., Harami, S.R.M., Ghorghani, N.F., Ganji, S., 2014. Distribution and ecological risk assessment of heavy metals in surface sediments along southeast coast of the Caspian Sea. *Mar. Pollut. Bull.* 81, 262–267.
- Blundell, A., Hannam, J.A., Dearing, J.A., Boyle, J.F., 2009. Detecting atmospheric pollution in surface soils using magnetic measurements: a reappraisal using an England and Wales database. *Environ. Pollut.* 57, 2878–2890.
- Chaparro, M.A.E., Sinito, A.M., 2004. An alternative experimental method to discriminate magnetic phases using IRM acquisition curves and magnetic demagnetisation by alternating field. *Rev. Bras. Geogr.* 22 (1):17–32. <http://dx.doi.org/10.1590/S0102-261X2004000100002>.
- Chaparro, M.A.E., Chaparro, M.A.E., Marinelli, C., Sinito, A.M., 2008a. Multivariate techniques as alternative statistical tools applied to magnetic proxies for pollution: cases of study from Argentina and Antarctica. *Environ. Geol.* 54, 365–371.
- Chaparro, M.A.E., Sinito, A.M., Ramasamy, V., Marinelli, C., Chaparro, M.A.E., Mullainathan, S., Murugesan, S., 2008b. Magnetic measurements and pollutants of sediments from Cauvery and Palaru River, India. *Environ. Geol.* 56, 425–437.

Table 1

Results from multivariate analysis, CA. Centroids for each group and corresponding magnetic parameters are detailed. Plus (+) and minus (–) indicate if the value is higher or lower than the overall mean. Asterisks (*) indicate that the centroid value is not different from the overall mean.

Magnetic parameter	G1	G2	G3	Overall mean
χ [$10^{-8} \text{ m}^3 \text{ kg}^{-1}$]	0.9(––)	9.3	81.4(++)	39.6
HIRM [$10^{-3} \text{ A m}^2 \text{ kg}^{-1}$]	0.01(––)	0.14	1.79(++)	0.84
H_{cr} [mT]	*****	64.5(––)	120.5(++)	90.1
ARM/SIRM [a.u.]	0.05(++)	*****	0.01(––)	0.02

- Chaparro, Marcos A.E., Chaparro, Mauro A.E., Rajkumar, P., Ramasamy, V., Sinito, Ana M., 2011. Magnetic parameters, trace elements and multivariate statistical studies of river sediments from south eastern India: a case study from Vellar River. *Environ. Earth Sci.* 63 (2), 297–310.
- Chaparro, M.A.E., Chaparro, M.A.E., Sinito, A.M., 2012. An interval fuzzy model for magnetic monitoring: estimation of a pollution index. *Environ. Earth Sci.* 66, 1477–1485.
- Chaparro, M.A.E., Suresh, G., Chaparro, M.A.E., Ramasamy, V., Sinito, A.M., 2013. Magnetic studies and elemental analysis of river sediments: a case study from the Ponnaiyar River (southeastern India). *Environ. Earth Sci.* 70, 201–213.
- Chaparro, M.A.E., Krishnamoorthy, N., Chaparro, M.A.E., Lecomte, Karina L., Mullainathan, S., Mehra, R., Sinito, Ana M., 2015a. Magnetic, chemical and radionuclide studies of river sediments and their variation with different physiographic regions of Bharathapuzha River, southwestern India. *Stud. Geophys. Geod.* 59, 438–460.
- Chaparro, M.A.E., Chaparro, M.A.E., Castañeda Miranda, A.G., Böhnelt, H.N., Sinito, A.M., 2015b. An interval fuzzy model for magnetic biomonitoring using the specie *Tillandsia recurvata* L. *Ecol. Indic.* 54, 238–245.
- Core Team, R., 2015. R: A Language and Environment for Statistical Computing. R Foundation for Statistical Computing, Vienna, Austria (URL <http://www.R-project.org/>).
- Dearing, J., 1999. Magnetic susceptibility. In: Walden, J., Oldfield, F., Smith, J. (Eds.), *Environmental Magnetism: A Practical Guide* Technical Guide No. 6. Quaternary Research Association, London, pp. 35–62.
- El-Bahi, S.M., 2004. Assessment of radioactivity and radon exhalation rate in Egyptian cement. *Health Phys.* 86, 517–522.
- El-Gamal, A., Nasr, S., El-Taher, A., 2007. Study of the spatial distribution of natural radioactivity in the upper Egypt Nile River sediments. *Radiat. Meas.* 42, 457–465.
- Evans, M.E., Heller, F., 2003. *Environmental Magnetism, Principles and Applications of Enviromagnetics*. Academic Press, New York 299 pp.
- Hanesch, M., Scholger, R., Dekkers, M.J., 2001. The application of fuzzy c-means cluster analysis and non-linear mapping to a soil data set for the detection of polluted sites. *Phys. Chem. Earth A* 26 (1–12), 885–891.
- Hong, C., Huh, C., Chen, K., Huang, P., Hsiung, K., Lin, H., 2009. Air pollution history elucidated from anthropogenic spherules and their magnetic signatures in marine sediments offshore of Southwestern Taiwan. *J. Mar. Syst.* 76, 468–478.
- King, J., Banerjee, S.K., Marvin, J., Özdemir, Ö., 1982. A comparison of different magnetic methods for determining the relative grain size of magnetite in natural materials: some results from lake sediments. *Earth Planet. Sci. Lett.* 59, 404–419.
- Krishnamoorthy, N., Mullainathan, S., Mehra, R., Chaparro, M.A.E., Chaparro, M.A.E., 2014. Radiation impact assessment of naturally occurring radionuclides and magnetic mineral studies of Bharathapuzha river sediments, South India. *Environ. Earth Sci.* 71, 3593–3604.
- Liu, Q., Roberts, A.P., Larrasoña, J.C., Banerjee, S.K., Guyodo, J., Tauxe, L., Oldfield, F., 2012. *Environmental magnetism: principles and applications*. *Rev. Geophys.* 50, RG4002. <http://dx.doi.org/10.1029/2012RG000393>.
- Bartington Instruments Ltd., 1994. Operation manual. *Environmental Magnetic Susceptibility – Using the Bartington MS2 System*. Chi Publishing, UK 54 pp.
- McCubbin, D., Leonard, K.S., Young, A.K., Maher, B.A., Bennett, S., 2004. Application of magnetic extraction technique to assess radionuclide-mineral association in Cumbrian shoreline sediments. *J. Environ. Radioact.* 77, 11–131.
- Montes, M.L., Mercader, R.C., Taylor, M.A., Runco, J., Desimoni, J., 2012. Assessment of natural radioactivity levels and their relationship with soil characteristics in undisturbed soils of the northeast of Buenos Aires province, Argentina. *J. Environ. Radioact.* 105, 30–39.
- Peters, C., Dekkers, M., 2003. Selected room temperature magnetic parameters as a function of mineralogy, concentration and grain size. *Phys. Chem. Earth* 28, 659–667.
- Petrovský, E., Ellwood, B., 1999. Magnetic monitoring of air, land and water pollution. In: Maher, B.A., Thompson, R. (Eds.), *Quaternary Climates, Environment and Magnetism*. Cambridge University Press, pp. 279–322.
- Petrovský, E., Kapicka, A., Jordanova, N., Boruka, L., 2001. Magnetic properties of alluvial soils contaminated with lead, zinc and cadmium. *J. Appl. Geophys.* 48, 127–136.
- Prajith, A., Rao, V.P., Kessarkar, P.M., 2015. Magnetic properties of sediments in cores from the Mandovi estuary, western India: inferences on provenance and pollution. *Mar. Pollut. Bull.* 99, 338–345.
- Ramasamy, V., Murugesan, S., Mullainathan, S., Chaparro, M.A.E., 2006. Magnetic characterization of recently excavated sediments of Cauvery River, Tamil Nadu, India. *Pollut. Res.* 25 (2), 357–362.
- Ramasamy, V., Sundararajan, M., Paramasivam, K., Meenakshisundaram, V., Suresh, G., 2013. Assessment of spatial distribution and radiological hazardous nature of radionuclides in high background radiation area, Kerala, India. *Appl. Radiat. Isot.* 73, 21–31.
- Ramasamy, V., Paramasivam, K., Suresh, G., Jose, M.T., 2014a. Role of sediments characteristics on natural radiation level of the Vaigai river sediment, Tamilnadu, India. *J. Environ. Radioact.* 127, 64–74.
- Ramasamy, V., Sundararajan, M., Suresh, G., Paramasivam, K., Meenakshisundaram, V., 2014b. Role of light and heavy minerals on natural radioactivity level of high background radiation area, Kerala, India. *Appl. Radiat. Isot.* 85, 1–10.
- Singh, H.N., Shanker, D., Neelakandan, V.N., Singh, V.P., 2007. Distribution patterns of natural radioactivity and delineation of anomalous radioactive zones using in situ radiation observations in Southern Tamil Nadu, India. *J. Hazard. Mater.* 141, 264–272.
- Song, Y., Choi, M.S., Lee, J.Y., Jang, D.J., 2014. Regional background concentrations of heavy metals (Cr, Co, Ni, Cu, Zn, Pb) in coastal sediments of the South Sea of Korea. *Sci. Total Environ.* 482–483, 80–91.
- Suresh, G., Ramasamy, V., Meenakshisundaram, V., Venkatachalapathy, R., Ponnusamy, V., 2011. Influence of mineralogical and heavy metal composition on natural radionuclide contents in the river sediments. *Appl. Radiat. Isot.* 69, 1466–1474.
- Suresh, G., Ramasamy, V., Sundararajan, M., Paramasivam, K., 2015. Spatial and vertical distributions of heavy metals and their potential toxicity levels in various beach sediments from high-background radiation area, Kerala, India. *Mar. Pollut. Bull.* 91 (1), 389–400.
- Thompson, R., Oldfield, F., 1986. *Environmental Magnetism*. Allen & Unwin (Publishers) Ltd. 225 pp.
- Tomlinson, D.L., Wilson, J.G., Harris, C.R., Jeffrey, D.W., 1980. Problems in the assessment of heavy metals levels in estuaries and the formation of a pollution index. *Helgoländer Meeresun.* 33, 566–575.
- Wang, X.-S., Qin, Y., 2006. Use of multivariate statistical analysis to determine the relationship between the magnetic properties of urban topsoil and its metal, S, and Br content. *Environ. Geol.* 51, 509–516.
- Yang, T., Liu, Q., Chan, L., Liu, Z., 2007. Magnetic signature of heavy metal pollution of sediments: case study from the East Lake in Wuhan, China. *Environ. Geol.* 52, 1639–1650.
- Zhang, C., Qiao, Q., Piper, J.D.A., Huang, B.B., 2011. Assessment of heavy metal pollution from a Fe-smelting plant in urban river sediments using environmental magnetic and geochemical methods. *Environ. Pollut.* 159, 3057–3070.